Pure & Appl. Chem., Vol. 64, No. 6, pp. 847–857, 1992.
Printed in Great Britain.

Applications of ESE spectroscopy in the study of electron spin polarization in bacterial photosynthesis

M.K. BOSCH, P. GAST AND A. J. HOFF

Department of Biophysics, Huygens Laboratory, University of Leiden
P.O. Box 9504, 2300 RA Leiden, The Netherlands

Abstract - In photosynthesis the photon energy of light is converted into chemical potential in the so-called Reaction Center (RC), a pigmented membrane protein that upon excitation gives rise to a charged radical pair. The radicals are spin correlated and in an external magnetic field the interactions (dipolar, exchange) between the two electron spins give rise to non-Boltzmann populations of their magnetic sublevels (spin polarization), which is probed by time-resolved EPR.

An overview is given of polarization phenomena in RC of bacterial origin, and recent theoretical interpretations highlighted. It is demonstrated that in all likelihood the exchange interaction of the primary radical pair in the RC of purple bacteria is positive. The implications of this result for our understanding of the initial processes of solar energy conversion are discussed.

1. PHOTOSYNTHETIC PHOTOCHEMISTRY

Photosynthesis is the conversion of the quantum energy of light by algae, higher plants and photosynthetic bacteria into the chemical energy of complex organic molecules and organized cellular structures. The light is absorbed by so-called antenna pigment-protein complexes, containing (bacterio)chlorophyll as their major pigment. The resulting electronic excited state is transferred among the antenna pigments by Förster resonant energy transfer until it is trapped by a specialized complex of (bacterio)chlorophyll, (B)Chl, molecules in a special protein, the reaction center (RC). In a few picoseconds, photochemistry on the excited specialized complex results in the donation of an electron to an electron acceptor, thus creating a pair of separated, charged radicals. Subsequent dark electron transport at either the donor or the acceptor side (or both) stabilizes the charges at the expense of free energy ("downhill" electron transport). Schematically:

$$\begin{aligned} &\text{Antenna} \xrightarrow{h\nu} \text{Antenna}^* \longrightarrow D^*A \xrightarrow[\lesssim 3\,\text{ps}]{} D^+A^- \\ &D_n \ldots D_1\, D^+A^-A_1 \ldots A_m \rightarrow D_n^+ \ldots D_1\, DAA_1 \ldots A_m^-. \end{aligned} \qquad (1)$$

Here D stands for donor and A for acceptor molecules, and the asterisk denotes an excited state.

In this contribution we will limit ourselves to the photosystem of BChl *a* containing purple bacteria as this is simpler and better understood than the photosystems of plants (or other photosynthetic bacteria). Moreover, the salient Electron Spin Polarization (ESP) phenomena can all be found in the first few steps of photochemistry in the reaction center of these particular bacteria.

1.1. Bacterial photosynthetic reaction centers

The primary photochemical reaction in the RC of BChl *a*-containing purple bacteria can be written as

$$P860^*\,.\,\text{Bph}\,a\,.\,Q \underset{}{\overset{<3\,\text{ps}}{\rightleftharpoons}} P860^+\,.\,\text{Bph}\,a^-\,.\,Q \overset{200\,\text{ps}}{\dashrightarrow} P860^+\,.\,\text{Bph}\,a\,.\,Q^- . \qquad (2)$$

Here P860 denotes the primary electron donor, a BChl *a* dimer having an absorption band at 860 nm, BPh the first electron acceptor, a bacteriopheophytin *a* (BChl *a* without the central Mg atom) molecule, and Q the secondary electron acceptor, a ubiquinone. It is convenient to abbreviate these labels to P, I and X, respectively.

When the secondary acceptor is reduced, either photochemically or by adding a chemical reductant, the electron of the primary reaction cannot pass to the ubiquinone, and the primary radical pair decays by

recombination, either to the singlet ground or excited state of P or to its triplet state, P^T:

$$P^* I X^- \rightleftharpoons P^+ I^- X^- \begin{cases} \rightarrow P^T I X^- \\ \rightarrow P I X^- \end{cases} \qquad (3)$$

In Eqn. 2 is indicated that the lifetime of the primary radical pair P^+I^- when X is not prereduced is about 200 ps. This time and the lifetime of the excited state P^*I depend very little on the temperature, so that it is possible to study the primary photochemistry at cryogenic temperatures, down to 1.5 K. In other words, the primary reaction of photosynthesis is a *solid state* reaction.

The complex machinery of the bacterial photosynthetic apparatus can be considerably simplified by isolating the RC protein from the photosynthetic membrane. The purified RC is fully capable of primary photochemistry. It has been crystallized and subjected to X-ray diffraction analysis, for which work J. Deisenhofer, R. Huber and H. Michel received in 1988 the Nobel prize for chemistry.[1] Their work, and subsequent similar work by the groups of Feher and Norris,[2,3] has allowed to draw a detailed picture of the spatial configuration of the active components and of some other co-factors. A schematized version is shown in Fig. 1. It is seen that there are two chains of pigment co-factors, each followed by a quinone molecule, in a C_2-symmetric arrangement. Surprisingly, only one chain, customarily labelled the A-chain, is photoactive, the second quinone molecule, Q_B, accepting the electron from Q_A^-. Q_B can be doubly reduced in two subsequent photoreactions, and when the RC is embedded in the photosynthetic membrane it leaves the RC to take part in further chemistry. In the isolated RC it is easily lost during the preparation procedure. The Q_A acceptor then cannot pass its electron further, and the charges on P^+ and Q_A^- recombine to the singlet state PIX in about 100 ms at room temperature and about 25 ms below 100 K. For RC having their full Q_B complement, electron transport from Q_A to Q_B is inhibited at lower temperatures and the P^+X^- pair decays by the same recombination reaction.

When Q_A is prereduced, or together with Q_B removed from the RC by extraction procedures, recombination of the photoproduced radical pair P^+I^- generates the triplet state P^TI with a yield of about 15% at 300 K and practically 100% at temperatures below 100 K. Under these conditions the lifetime of P^+I^- is 10-50 ns, depending somewhat on the temperature. The triplet state decays in a few μs at 300 K, and in about 100 μs below 100 K.

The many different redox states in which the RC can be prepared and the various regimes of radical pair lifetimes provide a rich playground for ESP enthusiasts. In the following Section a number of ESP observations for RC of the purple bacterium *Rhodobacter (Rb.) sphaeroides* strain R-26 will be discussed, some of which are unique and have as yet not been observed in vitro.

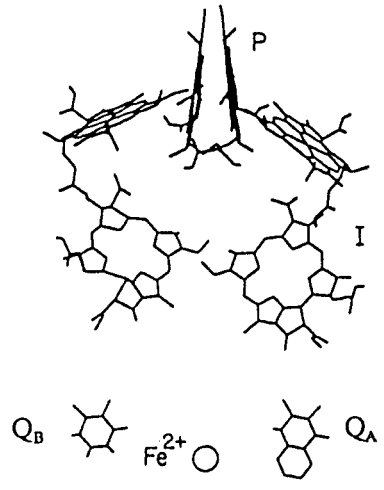

Fig. 1. Arrangement of the co-factors in the reaction center of *Rps. viridis*. Q_B is drawn symmetrically to Q_A, it is normally not seen by X-ray crystallography. Computed from coordinates obtained from Dr.J. Deisenhofer.

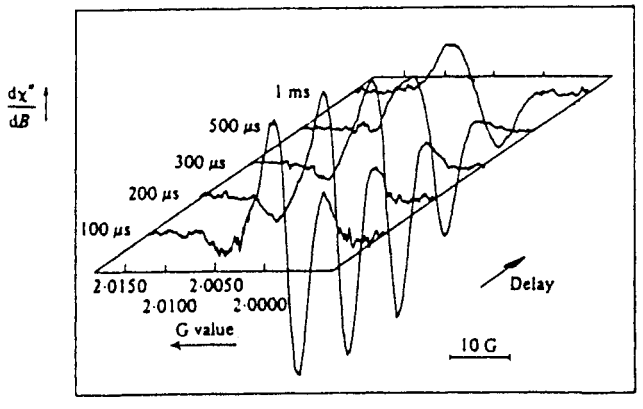

Fig. 2. Time-resolved flash EPR spectra of reaction centers of *Rb. sphaeroides* R-26 in which the quinone acceptor was magnetically decoupled from the iron. Delay times between the flash and the boxcar gate are indicated. From.[8]

2. ESP OF BACTERIAL PHOTOSYNTHETIC REACTANTS

Shortly after the first observation of ESP in plants,[4] ESP was observed in bacterial RC.[5] The latter observation showed conclusively that the Radical Pair Mechanism (RPM) and not the Triplet Mechanism (TM) was operative in generating ESP in (bacterial) photosynthesis. Further work showed that charge separation occurs from the singlet excited state, and that in all probability the exchange interaction J between P^+ and I^- is positive. Limiting values for both J and the z-component of the dipolar interaction between P^+ and X^-, D_{zz}, could be derived from extensive spectral simulation. In this Section a brief overview of ESP in the bacterial RC will be given, critically reviewing the information thus far gleaned.

2.1. ESP in active reaction centers

Unlike plants where ESP was observed without special treatment of the preparations, bacterial RC only showed ESP when they were subjected to detergent treatment.[5] It was shown that this was due to the abolishment of the magnetic interaction between the (first) quinone acceptor and the high spin ferrous ion that normally is present in the RC (Fig. 1). In "native" RC this interaction enormously broadens the EPR signal of Q_A^- and makes it a fast relaxer. The latter property presumably is responsible for the destruction of ESP in native RC. In later work it was demonstrated that the same ESP signals are observed when the RC are depleted of the ferrous ion,[6] but still functional with respect to primary photochemistry.[7]

The ESP signal depicted in Fig. 2 was recorded at 5 K with a cw X-band (9 GHz) EPR spectrometer having a time resolution of 20 μs, employing boxcar integration of the initial part of the decay curve following a laser flash. The polarized spectrum is shown at several delay times after the flash. At early times, the signal is maximally polarized (as confirmed by direct detection measurements with < 1 μs time resolution (A.J. Hoff and I.I. Proskuryakov, unpublished results). It decays within a few ms to the EPR signal in Boltzmann equilibrium, which consists of the overlapping EPR spectra of P^+ and Q_A^-.

2.2.1. *Simulated ESP spectrum for active RC: the RPM approach*

The maximally polarized experimental spectrum of Fig. 2 was simulated by Hore et al.[9] using the RPM formalism for ESP in the solid state, in which for the first time the dipolar interaction was correctly introduced. The simulation was based on the assumption that multiplet and net polarization is generated in the primary radical pair P^+I^-, and that subsequently the electron is transferred to Q_A, conserving only the net polarization of I^- (the information on the hyperfine couplings is lost upon transfer). The anisotropy of the dipolar interactions between P^+ and I^- and I^- and X^- (= Q_A^-), and of the g-value of X^- was averaged over all angles. It is seen from Fig. 3 that the agreement between experimental and simulated spectrum is quite good.

It is instructive to compare the different contributions to the lineshapes of polarized P^+ and X^- (Fig. 4). The net effect for P^+ is emissive, corresponding with $\Delta g < 0$ and a singlet precursor to $J < 0$. The multiplet pattern of P^+ (dashed line) agrees with this sign. The dipolar contribution to the lineshape of P^+ averages to zero. For

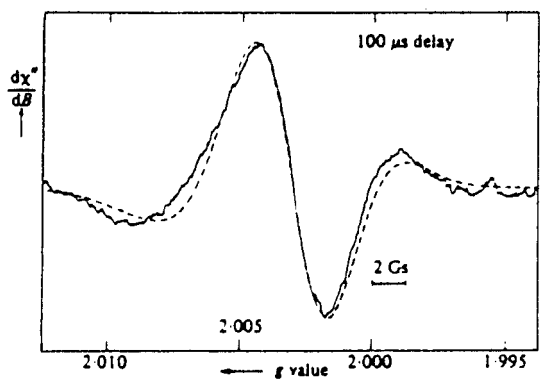

Fig. 3. Polarized spectrum of RC of *Rb. sphaeroides* at 5 K and a delay of 100 μs (Fig. 2) compared with a simulation based on the RPM[9] (broken line).

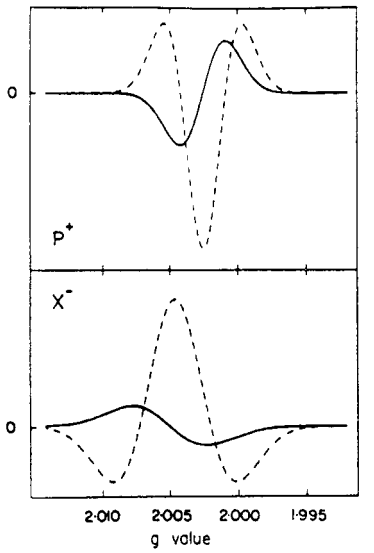

Fig. 4. The four contributions to the simulated spectrum of Fig. 3 corresponding to the net (solid line) and multiplet (broken line) ESP for P^+ and the net (solid line) and dipolar (broken line) components for X^-.[9]

X^- the net effect is absorptive, since now $\Delta g > 0$, and the multiplet effect is absent because of the electron transfer step. The dipolar interaction no longer averages to zero because of the anisotropic g-value of X^-. It is seen to dominate the lineshape of the polarized X^- signal and to be responsible for the emissive low field lobe of the total ESP spectrum. Would one have naively interpreted this lobe as the emissive part of a multiplet pattern of X^-, then the purported E/A pattern would have led to $J > 0$, the opposite of the sign of J used for the simulation.

Notwithstanding the success of the simulation a number of worrisome discrepancies remained. The linewidth of P^+ used for the simulation was almost half as small as that of the isolated P^+ in vivo (5.2 G vs. 9.7 G). The ratio $D_{P^+I^-}/J = 57$ derived from the best fit seemed very high compared with the value of $D_{P^+I^-}$ calculated from the crystal structure (– 5.5 G[8,10]) and the value of J estimated from a simulation of low-field Reaction Yield Detected Magnetic Resonance (RYDMAR) experiments, $|J| \sim 7$ G.[11,12] In addition, the intensity of the polarized signal, about three times that of the EPR spectrum in Boltzmann equilibrium, together with a lifetime of the P^+I^- pair of 250 ps requires $J \sim -80$ G, a value that is clearly much too large and not compatible with the quoted value for the ratio $D_{P^+I^-}/J$. A last and serious discrepancy was the g-value of I^- needed for the simulation, 2.0007 compared to $g = 2.0035$ for the BPh^- radical in vitro.

2.1.2. *Simulated ESP spectrum for active bacterial RC: the CRM approach*

The above difficulties with the classical RPM for explaining the ESP signal of active bacterial RC prompted Hore et al.[13] to take a radically different point of view. It was realized that an electron transfer time of 200 - 250 ps combined with a value of $|J_{PI}| < 10$ G is too short for generating appreciable polarization in the P^+I^- pair. In contrast, the magnetic interactions in the quasi-stable P^+X^- pair (lifetime ~ 25 ms at 5 K) might be strong enough for generating the required magnitude of CRM polarization. Thus, a simulation was undertaken using the Correlated Radicals Mechanism (CRM)[14,15] with sudden creation of the P^+X^- pair in the singlet state, taking into account the dipolar interaction between P^+ and X^- and the g-anisotropy of X^-. Averaging over all angles yielded the spectrum depicted in Fig. 5. It is seen that the correspondence between experimental and simulated spectrum is at least as good as for the earlier simulation based on the RPM. The parameter values, however, are now much more reasonable. The fit of Fig. 5 was obtained for $D_{P^+X^-} = -1.4$ G, $J_{P^+X^-} = 0$, literature values of the g-factor of P^+ and the g-tensor of X^-, and values for the angles defining the dipolar axis in the g-tensor coordinate frame of X^- that closely agreed with the values calculated from the crystal structure of RC of *Rhodopseudomonas (Rps.) viridis*,[1] which is homologous to that of *Rb. sphaeroides* R-26. The dipolar interaction agrees well with that found by De Groot et al.[16] for the triplet state of P and X^-; a small value of J is indicated by the large distance between P and X (about 3 nm). The calculated intensity of the ESP signal is about four times that of the corresponding equilibrium spectrum, in good agreement with the experimental ratio of about three.[17] The linewidth of X^- was identical to the literature value; that of P^+, however, was appreciably narrower (6.1 G vs. 9.4 G).

Comparing the results of the CRM simulation with that using the RPM approach, it appears that considerable progress is made in reconciling the values of the fit parameters to values derived from independent measurements. This lends credence to the validity of the CRM approach, but does not constitute proof. A point deserving further consideration is the lifetime of the P^+I^- pair, which was taken 200 ps as measured for native RC. For RC preparations that were depleted of the ferrous ion, however, it was reported[18] that the lifetime of P^+I^- rose to 4.2 ns, long enough for substantial RPM polarization to develop. Since the lifetime of P^+I^- in the preparations used for recording the ESP spectra of Fig. 2 is not known, simulations were undertaken combining the RPM and CRM in a rigorous way, following the procedures outlined in Ref. 6. It was found that for reasonable values of D_{PI} and J_{PI} no significant effects on the X-band ESP spectrum occurred for lifetimes of P^+I^- up to 1 ns.[16]

The question whether the ESP spectrum of RC of *Rb. sphaeroides* is due solely to the CRM or to an admixture of CRM and RPM could be answered if the lineshapes of the individual polarized radicals were known. In the following Section we will show that even at X-band such an unscrambling of complex overlapping ESP spectra can be achieved using a characteristic phenomenon of ESE spectroscopy, viz. that of *echo modulation*, or ESEEM.

2.1.3. *Modulation-discriminated echo spectroscopy of transient EPR (MODEST)*

Measuring the echo intensity as a function of τ yields the echo decay curve. Often this curve is not smooth but shows deep modulations. These arise from interference of allowed and forbidden transitions that are simultaneous excited by the intense microwave pulse. Fourier transformation of the modulated curve yields the

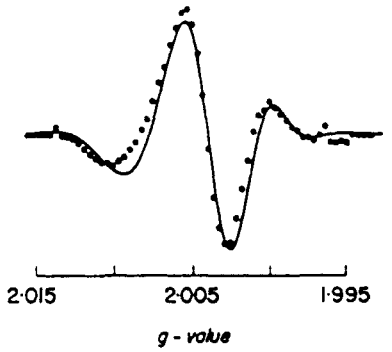

Fig. 5. Experimental ESP spectrum of Fig. 2 compared with a simulation based on the CRM.[13]

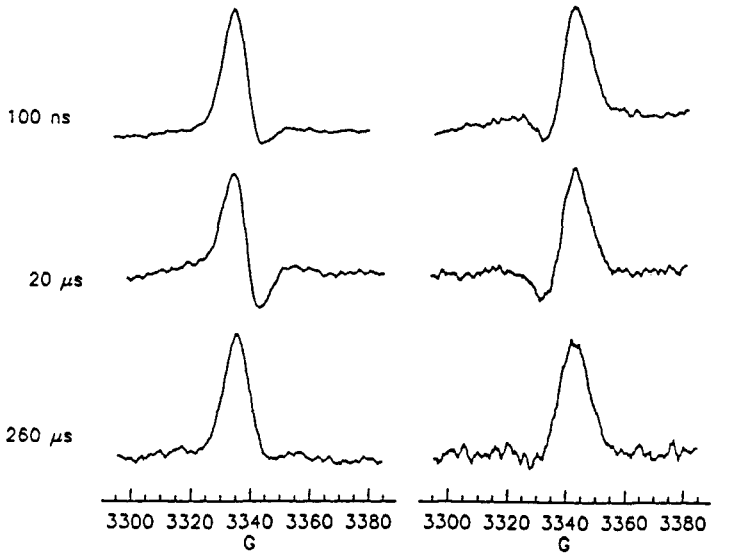

Fig. 6. MODEST spectra at 5 K of the radical pair P^+X^-. Lefthand column: τ = 325 ns, righthand column: τ = 1055 ns. Delay times as indicated.

hyperfine and/or quadrupole interactions (see for an introduction Mims and Peisach,[19] Dikanov and Astashkin,[20] and Schweiger.[21,22] Thus, the modulations constitute a fingerprint of the radical studied. Considering the two radicals of a photoinduced radical pair, it is often possible to select a value of τ for which one radical shows a maximum echo amplitude, whereas that of the other radical is practically zero. If the EPR spectra of these two radicals overlap, recording the echo amplitude for that particular value of τ as a function of the magnetic field (so-called *field-swept ESE*) then yields almost exclusively the spectrum of the first radical, that of the second being suppressed. If for another value of τ the situation is reversed, then recording again the field-swept spectrum for the second τ-value yields the spectrum of the second radical. We will call this technique, which has proved to be particularly useful in unscrambling complex overlapping ESP spectra of polarized radicals, MOdulation-Discriminated Echo Spectroscopy of Transient EPR signals, or MODEST.

When using the MODEST technique, care must be taken to first record the ESEEM curves of the individual, unperturbed radicals for selecting appropriate values of τ. Furthermore it has to be ascertained that the photoproduced radicals do not exhibit strong interactions. In addition, one must be aware of the possibility that together with electron spin polarization, the radicals may show nuclear spin polarization, which could affect the modulation pattern. Despite these caveats, MODEST is a powerful technique that allows measuring the ESP spectra of the individual radicals of a radical pair when the EPR spectra of these radicals overlap, as often happens in the solid state, even when employing high-frequency EPR.

Preliminary MODEST spectra of the radical pair P^+X^- are shown in Fig. 6. At τ = 325 and 1055 ns the modulation amplitude of P^+ and X^-, respectively, is practically zero and the isolated polarized spectrum of X^- or P^+ (left and right hand column, respectively) is recorded. It is seen that for short delay times after the laser flash the two spectra do not resemble the composite polarized spectrum of Fig. 2, indicating that good separation is indeed obtained. The spectrum of X^- conforms well to that expected from Fig. 4 (lower panel, the curves must be integrated). The polarized P^+ spectrum, however, deviates considerably from the expected curve; in fact the sum of the two spectra shows a net polarization not consistent with simple S - T_0 mixing. Note that the spectra are different from the simple CRM polarized spectra[14,15] because of the presence of anisotropic dipolar and g-tensors. The extensive calculations necessary for the interpretation of the spectra are currently underway.

2.1.4. *ESP of modified RC*

Further progress in understanding the ESP spectrum of bacterial RC was made by recording the spectrum at higher microwave frequency (Q-band, 35 GHz), using RC preparations that were subjected to either perdeuteration, and/or to extraction of the native quinone and reconstitution with perdeuterated or protonated quinones.[23] The ESP spectra were recorded using 500 Hz light modulation, and thus represent an integration of all the time-resolved spectra of Fig. 2. This makes them unsuitable for simulation attempts, but they are nevertheless valuable for qualitative considerations as they show a much better resolution of the spectral features

(Fig. 7) than the spectra previously obtained. Perdeuterated RC show the same X-band polarization pattern as previously observed (Fig. 2), viz. E/A/E/A, but the features are much sharper and the high-field lobe is more pronounced (Fig. 7a). The same pattern is observed at Q-band (Fig. 7b). RC reconstituted with perdeuterated quinone showed a polarized Q-band spectrum that was attributed to the perdeuterated quinone only, which is then completely in emission with peaks at the principal *g*-values (Fig. 7c). Perdeuterated RC reconstituted with protonated quinone showed a polarized Q-band spectrum that was attributed to the perdeuterated P^+ only, which then shows a A/E/A pattern (Fig. 7d). Superposition of the two polarized spectra indeed yielded a spectrum similar to that of perdeuterated native RC displayed in Fig. 7b.

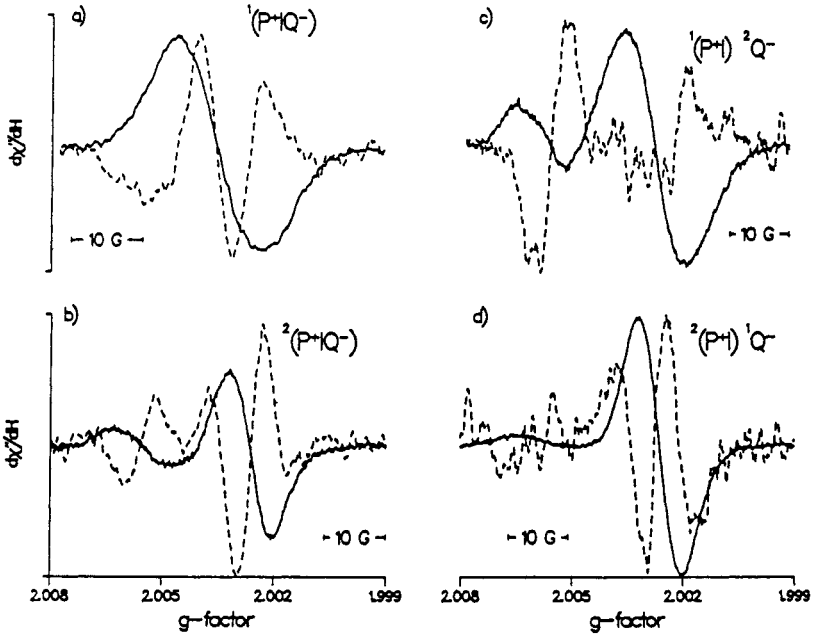

Fig. 7. Q-band EPR signal of RC of *Rb. sphaeroides* R-26 at 8 K (a) and 30 K (b,c,d) under continuous illumination (solid line) and 500 Hz light modulation (broken line).[23] Composition of the RC as indicated.

The interpretation with the conventional RPM supplemented with polarization transfer yields an X-band polarized spectrum with an A/E pattern (Fig. 4). At Q-band one would expect this pattern to change to predominantly net, emissive polarization (Fig. 4), since then the multiplet contribution is expected to be much smaller than the contribution due to the difference in Zeeman splitting. Experimentally one observes an A/E/A pattern at Q-band. Thus, it appears that polarization transfer alone cannot explain the ESP signals of active RC, in agreement with the rather satisfactory simulation of the X-band ESP spectrum by Hore et al.,[15] which was based on the assumption that solely CRM polarization of the pair P^+X^- contributes. As mentioned by Hore et al.,[15] in reality iron-depleted RC may exhibit a lifetime of P^+I^- that is long enough (> 1 ns) for significant polarization to build up. Simulations of ESP spectra of RC with *known* P^+I^- lifetime are obviously needed to sort this out. Feezel et al.[23] have demonstrated that by carrying out such experiments on perdeuterated material at Q-band, a much higher resolution and therefore better discrimination of the simulations can be achieved.

2.2 ESP in blocked reaction centers

2.2.1. *Experimental results*

As discussed in Section 1.1. the secondary quinone acceptor can be prereduced, thereby blocking forward electron transport. The lifetime of the photoinduced P^+I^- pair is then considerably enhanced compared to that in active RC (viz. 20-50 ns vs. 200-250 ps), allowing ample time for singlet-triplet mixing. The pair decays through recombination to either the singlet excited or ground state of P or to its triplet state, P^T. As a result of magnetic interactions between the reduced secondary acceptor X^- and the CRM polarized P^+I^- pair, polarization is transferred to X^- with a lifetime corresponding to the spin-lattice relaxation time of X^-. During this time the P^+I^- pair may turn over several times, "pumping" polarization into X^-. The result is striking[24] (Fig. 8): at 5 K under intense illumination the normal, absorptive cw EPR signal of X^- becomes completely emissive! Because of the "pumping" action one would expect that the emissivity depends on the intensity of the illumination.

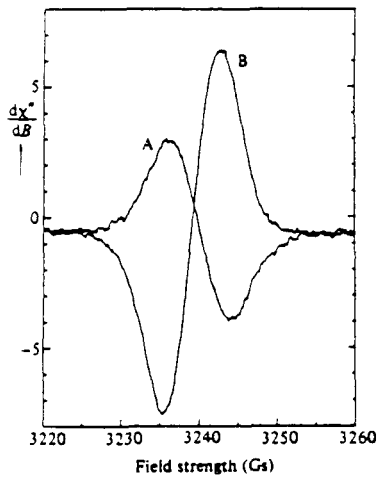

Fig. 8. Dark EPR spectrum of X^- of RC of *Rb. sphaeroides* at 5 K (trace A) and the spectrum under continuous illumination (trace B).[24]

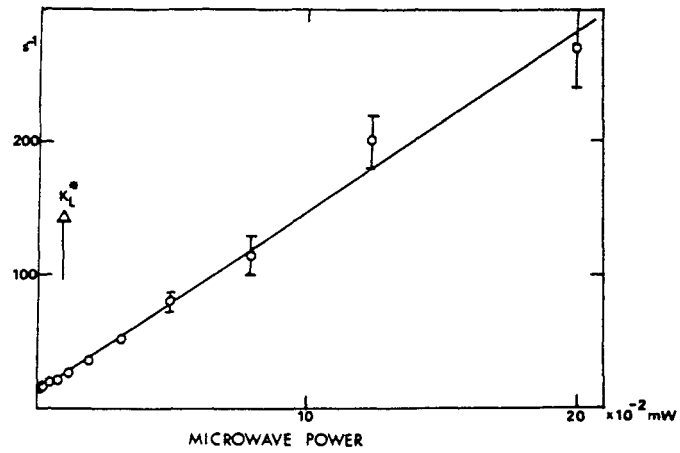

Fig. 9. Plot of the light flux at which the amplitude of the light-induced emissive signal of Fig. 14 is half-saturated as a function of the microwave power.[24]

Moreover, it should inversely depend on the microwave power. Both predictions were verified. In Fig. 9 the microwave power is plotted against the half-saturation light intensity k_L^*, at which half the maximum emissivity is attained. Simple kinetic considerations based on the scheme of Fig. 10 predict a linear relationship[24], as observed.

In spite of the success of the phenomenological description of the generation of emissive polarization of X^-, one observation remained unexplained. The emissive signal of Fig. 8 clearly shows a *g*-shift with respect to the dark signal, which depended on the microwave power. The *g*-shift is surprising as one would expect that an emissive, net-polarized signal (the transfer should be independent of nuclear spin) would faithfully reproduce the original lineshape. Possible explanations include the deformation of a true net-polarized signal of X^- by relaxation phenomena, emissive polarization of a radical other than X^-, and a polarization process more involved than simple transfer of polarization, which should then be non-uniform across the line of X^-. This phenomenon was therefore studied in detail with ESE spectroscopy, which technique is free from the microwave power dependence and allows to record the T_1 and T_2 relaxation times across the X^- line.[7] In addition, using the ESEEM option it is possible to unequivocally identify the polarized signal by recording its "fingerprint" echo modulation and comparing it to that of the dark signal.

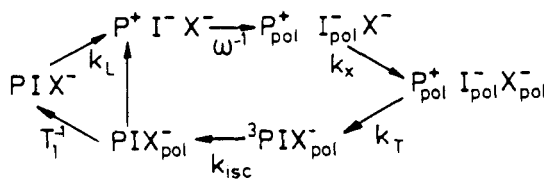

Fig. 10. Kinetic scheme of the "pumping" cycle for the generation of polarization in X^-.[6]

The results of the ESE study are summarized in Fig. 11. In panel (a), the ESEEM traces of the emissive signal (inverted for clarity) and the dark signal are compared. It is seen that they are identical, positively identifying the emissive signal as due to X^-. In panel (b) the T_1 relaxation time, measured with a three-pulse sequence, is depicted as a function of magnetic field. The small dependence on field position within the line is symmetric and cannot explain the *g*-shift. This was confirmed comparing a medium-polarized signal (medium-intensity light flash) recorded directly after the flash with a signal produced with maximal polarization (saturating light flash) and recorded 1 s after the flash (Fig. 11c). The clearly non-uniformly polarized signal directly after the flash is identical with that recorded after the polarization has partly decayed, excluding that the non-uniform polarization is due to an anisotropic T_1. In panel (d) the dark and emissive signals are compared for different echo-delay times 2τ. The *g*-shift is preserved over most of the echo decay period, excluding anisotropic T_2 as a possible source of the *g*-shift.

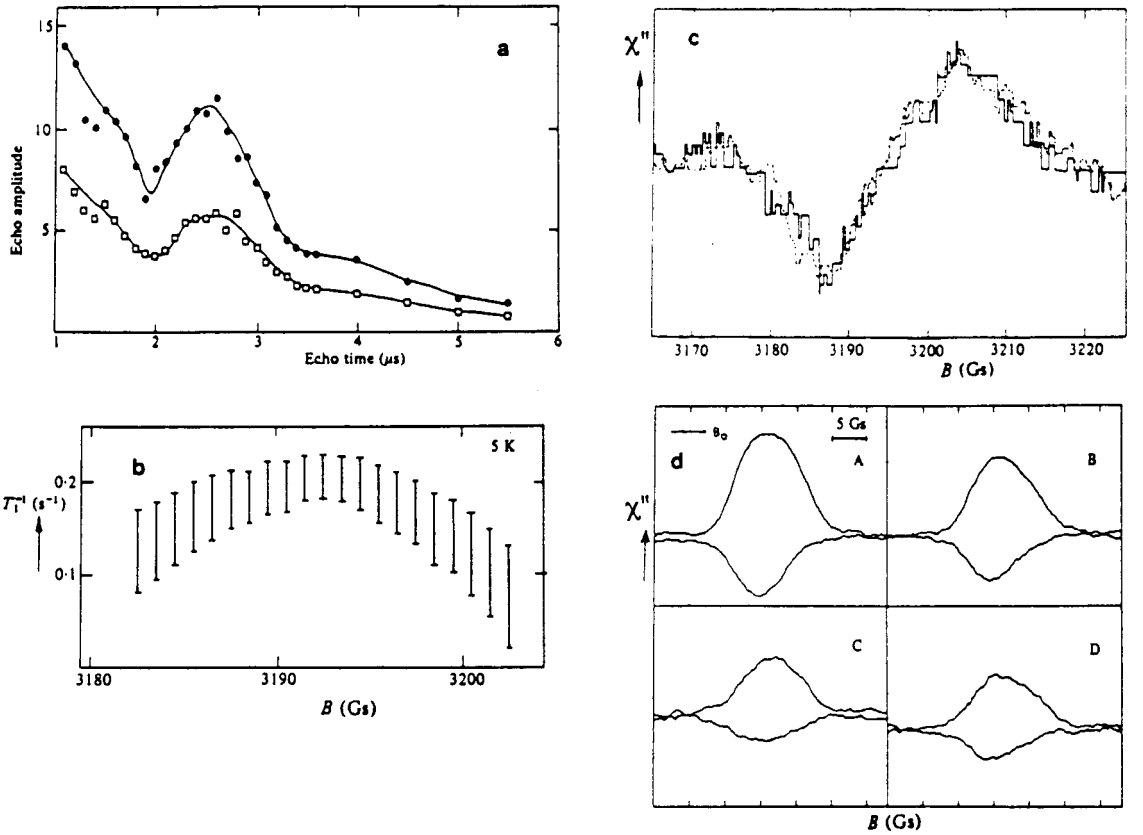

Fig. 11. (a) Echo-modulation envelope of the absorptive ESE signal of X^- at 5 K in the dark (open squares) and of the emissive signal under continuous illumination (filled circles, sign inverted)[7].
(b) Spin-lattice relaxation time of the emissive signal at 5 K as a function of magnetic field. Bars represent 90% error limits.[7]
(c) Partially polarized ESE spectra of X^- at 5 K. Solid line: 1 ms after light flash of reduced intensity; broken line: 2 s after light flash of saturating intensity.[7] Note that χ'' is monitored.
(d) ESE spectra of the dark (upper traces) and emissive (lower traces) signals of X^- at 5K for different echo delay times 2τ of 1.1 (A), 1.5 (B), 2 (C) and 4 (D) μs.[7]

The remaining explanation, an inherent non-uniformity of the polarization mechanism, was investigated employing high-frequency (Q-band) EPR and perdeuterated material, thus allowing much greater resolution.[25] The dark and polarized spectra are displayed in Fig. 12. At the g_z and g_x positions, the line becomes emissively polarized, whereas at g_y there is almost no polarization. Clearly, the polarization mechanism is strongly dependent on the orientation of the X acceptor with respect to the magnetic field. This immediately suggests that the dipolar interaction between I^- and X^- and/or between P^+ and X^- plays a dominant role,[9] and prompted Hore et al.[26] to undertake a simulation of the polarized signal at Q-band, to which work we will now turn.

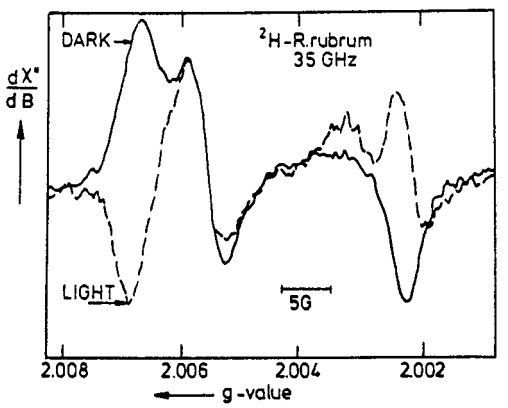

Fig. 12. Q-band spectrum of X^- in perdeuterated SDS-treated cells of *R. rubrum* at 80 K in the dark (solid line) and under continuous illumination of saturating intensity (broken line).[25]

2.2.2. *Calculation of polarization in the three-spin system $P^+I^-X^-$*

In a first attempt to calculate the polarization of X^- in the $P^+I^-X^-$ three-spin system, Hoff and Hore[27] used the formalism of Stochastic Liouville Equation (SLE) with isotropic *g*-values, varying the values of the two exchange and the two dipolar couplings. (Those between P^+ and X^- were neglected.) It was found that for the parameters values searched, emissive polarization resulted only when $J_{PI} > 0$. A more extended parameter search revealed that weak emissivity occurs for $J_{PI} \approx -5$ G, $J_{IX} \approx -10$ G.[28] Clearly, just the sign of the polarized X-band spectrum of X^- is not a sufficiently discriminatory criterium.

To shed more light on the sign of J_{PI}, Hore et al.[26] undertook a simulation of the well-resolved spectrum of Fig. 12, incorporating the anisotropic *g*-tensor of X^-. Since simulating the complete spectrum with variation of the large number of parameters, including the angles defining the position of the dipolar axes with respect to the *g*-tensor coordinate frame of X^-, over a considerable range would have been prohibitively demanding on computer time, it was decided to take as criteria for a successful fit the inequalities

$$3\Phi_z \geq \Phi_x \geq \Phi_z \geq 0.01$$
$$\Phi_z \geq 3\Phi_y \geq -\Phi_z \qquad (4)$$

i.e. somewhat more emission is found at g_x than at g_z, while that at g_y is much smaller. In addition the directions of the two dipolar axes were restricted to be parallel to one of the principal axes of the *g*-tensor of X^- (X, Y, and Z). From an extensive parameter search during which more than 270.000 sets of polarizations were calculated, three general conclusions could be derived:

i. The X^- polarization is not sensitive to either the magnitude and direction of the P^+I^- *dipolar* coupling or to the magnitude and sign of the I^-X^- *exchange* interaction. Thus, both the magnitude *and* the anisotropy of the polarization must come from D_{IX}, whose absolute value indeed has to be larger than 5 G to generate the required polarization.

ii. $k_T \geq 2 \cdot 10^8$ s^{-1} and $k_S \leq 8 \cdot 10^7$ s^{-1}.

iii. The magnitude and sign of the *exchange* interaction between P^+ and I^- are correlated with the direction of the I^-X^- dipolar axis:

$$\begin{aligned} &J_{PI} \leq -4 \text{ G } \textit{and } \Gamma_{IX} = \text{X } \textit{or } \text{Z} \\ &-4 \text{ G} \leq J_{PI} \leq +4 \text{ G } \textit{and } \Gamma_{IX} = \text{X } \textit{or } \text{Y } \textit{or } \text{Z} \\ &J_{PI} \geq +4 \text{ G } \textit{and } = \text{Y}, \end{aligned} \qquad (5)$$

where Γ_{IX} indicates the direction of the dipolar axis between I^- and X^-. For $|J_{PI}| \geq 4$ G, successful simulations with Γ_{IX} = Y were 30-fold more numerous than those with the first condition of Eqn. 5. The three above conclusions were insensitive to the addition of an average hyperfine coupling, agreeing with the notion that at 35 GHz the differences in Zeeman interaction dominate.

From the crystal structure of *Rb. sphaeroides* R-26[2] and data on the *g*-tensors of model quinones,[29,30] one finds that the direction of D_{IX} is roughly parallel to the Y axis. The modulus of J_{PI} as obtained from RYDMAR experiments and measurements of the effect of a magnetic field on the yield of P^T falls within fairly narrow limits: 5 G $\leq |J_{PI}| \leq$ 8 G.[12,31,32] It follows that only the last option of Eqn. 5 can explain the observed polarization pattern of Fig. 12 and that consequently J_{PI} is *positive*. The implications of this discovery for our understanding of primary electron transport in the RC will now be discussed.

3. RELEVANCE OF THE EXPERIMENTAL RESULTS FOR ELECTRON TRANSPORT THEORY

The mechanism of charge separation in bacterial RC is presently heavily debated. Two competing mechanisms have been proposed. Firstly, the so-called two-step mechanism, in which the accessory BChl, B_A, is reduced for a finite time before I is reduced.[33,34,35] Secondly, the so-called superexchange mechanism in which B_A mediates electron transfer by coupling to both P and I, but is not reduced itself.[36,37] Obviously, the relative importance of the two mechanisms depends on the position of the energy level of $P^+B_A^-$: if it lies well below that of P^*, then the two-step mechanism is operative, if it lies well above P^*, then the superexchange mechanism governs charge separation. Experimental evidence pro and contra the two proposed mechanisms is accumulating, but until now no consensus has been reached.[38,39,40]

The energy difference between P^* and $P^+B_A^-$, ΔG_1, controls the energy of the singlet state of the radical pair, $^1[P^+I^-]$, but not the energy of its triplet state, $^3[P^+I^-]$. Therefore, knowledge of the magnitude and sign of the singlet-triplet splitting of P^+I^-, $2J_{PI}$, would in principle allow an assessment of magnitude and sign of ΔG_1, hence of the importance of the superexchange vs. the sequential two-step model. Bixon et al.[37] calculated $2J_{PI}$ as the difference in the energy shifts of the singlet and triplet state of P^+I^-, due to interactions with P^* and P^T:

$$2J_{PI} = \delta E_S(P^*) - \delta E_T(P^T) . \qquad (6)$$

The two terms of Eqn. 6 are of comparable magnitude, have the same sign and practically cancel. Moreover, $\delta E_S(P^*)$ depends on the square of a reduction factor b that takes into account a possible relaxation of the nuclear configuration of P^+I^- following its formation from P^*.[36] This means that the sign and magnitude of $2J_{PI}$ critically depends on *both* the position of the energy level of $P^+B_A^-$ relative to P^* *and* the value of b.

Assuming that $P^+B_A^-$ lies 600 cm^{-1} above P^* and using $|2J_{PI}| = 10^{-3}$ cm^{-1}, Bixon et al.[37] found that $0.4 < b < 0.6$. The present work indicates that $2J$ is positive and has the value $2J = +14 \pm 1$ G ($+1.3 \pm 0.1$ cm^{-1}), which with the same value of ΔG_1 yields $0.33 < b < 0.36$.

The narrow range of possible values of b that results from the determination of the sign of J_{PI} suggests that either the assumed value of ΔG_1 is precisely correct, which would be surprising in view of the many approximations involved,[37] or that this energy difference needs adjustment so that the precise value of b is less critical.

Bixon et al.[41] recently explored the consequences of varying ΔG_1 between -800 cm^{-1} ($P^+B_A^-$ below P^*) and $+500$ cm^{-1} ($P^+B_A^-$ above P^*). Four ranges were defined: (I) $\Delta G_1 \leq -400$ cm^{-1}; sequential two-step mechanism at all temperatures, (II) -400 $cm^{-1} \leq \Delta G_1 \leq 0$; superposition of sequential and superexchange mechanisms at all temperatures, (III) $0 \leq \Delta G_1 \leq +400$ cm^{-1}; superposition of sequential and superexchange mechanisms at room temperature and superexchange mechanism at low temperature (100 K), (IV) $\Delta G_1 \geq +400$ cm^{-1}; superexchange mechanism at all temperatures. Utilizing Eqn. 6 with somewhat different values of the reorganization energies than in their previous calculation[37] and taking $b = 1$, the authors found that over the range $\Delta G_1 = -600$ cm^{-1} to 0 the calculated value of $2J_{PI}$ was in accord with the experimental value of $|2J_{PI}|$. In other words, it was probable that the superexchange and sequential mechanism coexist at all temperatures, but a sequential mechanism at all temperatures could not be excluded.

The finding by Hore et al.[26] that J_{PI} is positive allows to narrow down the permissible values of ΔG_1 considerably. Taking the same parameter values as in Bixon et al.[41] one finds for $J_{PI} > 0$, $\Delta G_1 \leq -100$ cm^{-1}; for $2J_{PI} = +1.3 \cdot 10^{-3}$ cm^{-1}, $\Delta G_1 = -200$ cm^{-1}. Thus, at all temperatures the sequential and superexchange mechanisms operate in parallel. Note that this agrees with the temperature independence of the abolute value of J_{PI} as found in [11].

As pointed out by Bixon et al.,[41] the "peaceful coexistence" of the two routes for primary electron transport makes the primary process robust with regard to moderate variations of the energetic parameters. This, obviously, must have been of prime importance in the evolution of the various photosystems.

The above conclusion is valid for values of the reduction factor b, which lowers the contribution of $\delta E_S(P^*)$ to $2J_{PI}$, that are close to unity. If b is much smaller, then $\delta E_S(P^*)$ and consequently ΔG_1 are appreciably larger. For example, for $b = 0.5$, $\Delta G_1 = 20 - 30$ cm^{-1}, favoring the superexchange mechanism at low temperatures. At physiological temperatures, however, and excepting values of b much smaller than 0.5, the parallelism of the two electron transport routes seems now well established.

4. PROSPECTS

In this report we have endeavoured to highlight the contribution that time-resolved EPR can make to the elucidation of the fundamental mechanisms of primary electron transport in bacterial photosynthesis. Much of what has been discussed is also applicable to the plant photosystems,[42] be it in lesser detail. As mentioned, more work has to be done to firm up the conclusions. Conjunction of time-resolved EPR and optical spectroscopies is indispensable to allow extraction of meaningful values of the magnetic interactions between the various electron transport components. It is desirable to perform experiments on oriented samples in order to separate the contributions of the exchange and dipolar interactions. The work on the plant photosystems has to be extended, especially on the RC of Photosystem II, which although thought to be homologous to the bacterial RC, shows quite different behavior with respect to ESP phenomena. For all photosystems, work at higher frequencies with (per)deuterated material will considerably improve resolution and therefore narrow the limits of confidence for the parameters extracted from the simulation of ESP spectra. Finally, artificial systems modelling the photosynthetic transport chains should be screened for their potential to mimic the spin polarization behavior of the in vivo systems.[43]

Acknowledgements

The work done in Leiden was supported by the Netherlands Foundation for Chemical Research (SON), financed by the Netherlands Organization for Scientific Research (NWO).

REFERENCES

1. J. Deisenhofer, O. Epp, K. Miki, R. Huber and H. Michel, *Nature* **318** (1985) 618-624.
2. J.P. Allen, G. Feher, T.O. Yeates, D.C. Rees, J. Deisenhofer, H. Michel and R. Huber, *Proc. Natl. Acad. Sci. USA* **83** (1986) 8589-8593.
3. C.H. Chang, D. Tiede, J. Tang, U. Smith, J. Norris and M. Schiffer, *FEBS Lett.* **205** (1986) 82-86.
4. R. Blankenship, A. McGuire and K. Sauer, *Proc. Natl. Acad. Sci. USA* **72** (1975) 4943-4947.
5. A.J. Hoff, P. Gast and J.C. Romijn, *FEBS Lett.* **73** (1977) 185-190.
6. A.J. Hoff, *Quart. Rev. Biophys.* **17** (1984) 153-282.
7. P. Gast, R.A. Mushlin and A.J. Hoff, *J. Phys. Chem.* **86** (1982) 2886-2891.
8. R.J. Debus, G. Feher and M.Y. Okamura, *Biochemistry* **25** (1986) 2276-2287.
9. P.J Hore, E.T. Watson, J.B. Pedersen and A.J. Hoff, *Biochim. Biophys. Acta* **849** (1986) 70-76.
10. A. Ogrodnik, W. Lersch, M.E. Michel-Beyerle, J. Deisenhofer and H. Michel, in *Antennas and Reaction Centres of Photosynthetic Bacteria*, ed. M.E. Michel-Beyerle (Springer Verlag, Berlin, 1985) pp. 198-206.
11. K.W. Möhl, E.J. Lous and A.J. Hoff, *Chem. Phys. Lett.* **121** (1985) 22-27.
12. D.A. Hunter, A.J. Hoff and P.J. Hore, *Chem. Phys. Lett.* **134** (1987) 6-11.
13. P.J. Hore, D.A. Hunter, C.D. McKie and A.J. Hoff, *Chem. Phys. Lett.* **137** (1987) 495-500.
14. C.D. Buckly, D.A. Hunter, P.J. Hore, and K.A. McLauchlan, *Chem. Phys. Lett.* **135** (1987) 307-312.
15. G.L. Closs, M.D.E. Forbes and J.R. Norris, *J. Phys. Chem.* **91** (1987) 3592-3599.
16. A. de Groot, P. Gast and A.J. Hoff, *Biochim. Biophys. Acta* **808** (1985) 13-20.
17. P. Gast, *Doctoral Dissertation* (Leiden, 1982).
18. C. Kirmaier, D. Holten, R.J. Debus, G. Feher and M.Y. Okamura, *Proc. Natl. Acad. Sci. USA* **83** (1986) 6407-6411.
19. W.B. Mims and J. Peisach, in *Advanced EPR. Applications in Biology and Biochemistry*, ed. A.J. Hoff (Elsevier, Amsterdam, 1989) pp. 1-57.
20. S.A. Dikanov and A.V. Astashkin, in *Advanced EPR. Applications in Biology and Biochemistry*, ed. A.J. Hoff (Elsevier, Amsterdam, 1989) pp. 59-117.
21. A. Schweiger, in *Advanced EPR. Applications in Biology and Biochemistry*, ed. A.J. Hoff (Elsevier, Amsterdam, 1989) pp. 277-305.
22. A. Schweiger, *Angew. Chem. Int. Ed. Engl.* **30** (1991) 265-292.
23. L.L. Feezel, P. Gast, U.H. Smith and M.C. Thurnauer, *Biochim. Biophys. Acta* **974** (1989) 149-155.
24. P. Gast and A.J. Hoff, *Biochim. Biophys. Acta* **548** (1979) 520-535.
25. P. Gast, A. de Groot and A.J. Hoff, *Biochim. Biophys. Acta* **723** (1983) 52-58.
26. P.J. Hore, D.J. Riley, J.J. Semlyen and A.J. Hoff, *Biochim. Biophys. Acta* in the press.
27. A.J. Hoff and P.J. Hore, *Chem. Phys. Lett.* **108** (1984) 104-110.
28. P.J. Hore, in *Advanced EPR. Applications in Biology and Biochemistry*, ed. A.J. Hoff (Elsevier, Amsterdam, 1989) pp. 405-440.
29. B.J. Hales, *J. Amer. Chem. Soc.* **97** (1975) 5993-5997.
30. O. Burghaus, *Doctoral Dissertation* (Berlin, 1991).
31. J.R. Norris, C.P. Lin and D. Budil, *J. Chem. Soc. Faraday I* **83** (1987) 13-27.
32. W. Lersch, F. Lendzian, E. Lang, R. Feick, K. Möbius and M.E. Michel-Beyerle, *J. Magn. Res.* **82** (1989) 143-149.
33. R. Haberkorn, M.E. Michel-Beyerle and R.A. Marcus, *Proc. Natl. Acad. Sci. USA* **70** (1979) 4185-4188.
34. R.A. Marcus, *Chem. Phys. Lett.* **133** (1987) 471-477.
35. R.A. Marcus, *Chem. Phys. Lett.* **146** (1988) 13-22.
36. M.E. Michel-Beyerle, M. Bixon and J. Jortner, *Chem. Phys. Lett.* **151** (1988) 188-194.
37. M. Bixon, J. Jortner, M.E. Michel-Beyerle and A. Ogrodnik, *Biochim. Biophys. Acta* **977** (1989) 273-286.
38. J. Breton, J.-L. Martin, G.R. Fleming and J.-C. Lambry, *Biochemistry* **27** (1988) 8276-8284.
39. W. Holzapfel, U. Finkele, W. Kaiser, D. Oesterhelt, H. Scheer, H.U. Stilz and W. Zinth, *Chem. Phys. Lett.* **160** (1989) 1-7.
40. C. Kirmaier and D. Holten, *Proc. Natl. Acad. Sci. USA* **87** (1990) 3552-3556.
41. M. Bixon, J. Jortner and M.E. Michel-Beyerle, *Biochim. Biophys. Acta* **1056** (1991) 301-315.
42. D. Stehlik, C.H. Bock and M.C. Thurnauer, in *Advanced EPR. Applications in Biology and Biochemistry*, ed. A.J. Hoff (Elsevier, Amsterdam, 1989) pp. 371-403.
43. M.R. Wasielewski, G.L. Gaines, M.P. Oneil, W.A. Svec and M.P. Niemczyk, *Mol. Cryst. Liq. Cryst.* **194** (1991) 201-207.